Mapping the local dielectric response at the nanoscale by means of plasmonic force spectroscopy

Francesco De Angelis,* Remo Proietti Zaccaria, and Enzo Di Fabrizio

Istituto Italiano di Tecnologia, via Morego 30, 16163 Genova, Italy
francesco.deangelis@iit.it

Abstract: At the present, the local optical properties of nanostructured materials are difficult to be measured by available instrumentation. We investigated the capability of plasmonic force spectroscopy of measuring the optical response at the nanoscale. The proposed technique is based on force measurements performed by combining Atomic Force Microscopy, or optical tweezers, and adiabatic compression of surface plasmon polaritons. We show that the optical forces, caused by the plasmonic field, depend on the local response of the substrates and, in principle, allow probing both the real and the imaginary part of the local permittivity with a spatial resolution of few nanometers.

OCIS codes: (240.6680) Surface plasmons; (310.6628) Subwavelength structures, nanostructures; (180.5810) Scanning microscopy.

References and links

1. M. L. Juan, M. Righini, and R. Quidant, "Plasmon nano-optical tweezers," Nat. Photonics **5**(6), 349–356 (2011).
2. L. Novotny, R. X. Bian, and X. S. Xie, "Theory of nanometric optical tweezers," Phys. Rev. Lett. **79**(4), 645–648 (1997).
3. P. C. Chaumet, A. Rahmani, and M. Nieto-Vesperinas, "Optical trapping and manipulation of nano-objects with an apertureless probe," Phys. Rev. Lett. **88**(12), 123601 (2002).
4. M. Righini, A. S. Zelenina, C. Girard, and R. Quidant, "Parallel and selective trapping in a patterned plasmonic landscape," Nat. Phys. **3**(7), 477–480 (2007).
5. C. Chen, M. L. Juan, Y. Li, G. Maes, G. Borghs, P. Van Dorpe, and R. Quidant, "Enhanced optical trapping and arrangement of nano-objects in a plasmonic nanocavity," Nano Lett. **12**(1), 125–132 (2012).
6. J. R. Arias-González and M. Nieto-Vesperinas, "Optical forces on small particles: attractive and repulsive nature and plasmon-resonance conditions," J. Opt. Soc. Am. A **20**(7), 1201–1209 (2003).
7. F. De Angelis, G. Das, P. Candeloro, M. Patrini, M. Galli, A. Bek, M. Lazzarino, I. Maksymov, C. Liberale, L. C. Andreani, and E. Di Fabrizio, "Nanoscale chemical mapping using three-dimensional adiabatic compression of surface plasmon polaritons," Nat. Nanotechnol. **5**(1), 67–72 (2010).
8. F. De Angelis, M. Patrini, G. Das, I. Maksymov, M. Galli, L. Businaro, L. C. Andreani, and E. Di Fabrizio, "A hybrid plasmonic-photonic nanodevice for label-free detection of a few molecules," Nano Lett. **8**(8), 2321–2327 (2008).
9. A. Weber-Bargioni, A. Schwartzberg, M. Cornaglia, A. Ismach, J. J. Urban, Y. Pang, R. Gordon, J. Bokor, M. B. Salmeron, D. F. Ogletree, P. Ashby, S. Cabrini, and P. J. Schuck, "Hyperspectral nanoscale imaging on dielectric substrates with coaxial optical antenna scan probes," Nano Lett. **11**(3), 1201–1207 (2011).
10. C. C. Neacsu, S. Berweger, R. L. Olmon, L. V. Saraf, C. Ropers, and M. B. Raschke, "Near-field localization in plasmonic superfocusing: a nanoemitter on a tip," Nano Lett. **10**(2), 592–596 (2010).
11. S. Berweger, J. M. Atkin, X. G. Xu, R. L. Olmon, and M. B. Raschke, "Femtosecond nanofocusing with full optical waveform control," Nano Lett. **11**(10), 4309–4313 (2011).
12. N. C. Lindquist, P. Nagpal, A. Lesuffleur, D. J. Norris, and S. H. Oh, "Three-dimensional plasmonic nanofocusing," Nano Lett. **10**(4), 1369–1373 (2010).
13. A. Weber-Bargioni, A. Schwartzberg, M. Schmidt, B. Harteneck, D. F. Ogletree, P. J. Schuck, and S. Cabrini, "Functional plasmonic antenna scanning probes fabricated by induced-deposition mask lithography," Nanotechnology **21**(6), 065306 (2010).
14. J. Kohoutek, D. Dey, A. Bonakdar, R. Gelfand, A. Sklar, O. G. Memis, and H. Mohseni, "Opto-mechanical force mapping of deep subwavelength plasmonic modes," Nano Lett. **11**(8), 3378–3382 (2011).
15. J. F. Song, R. P. Zaccaria, G. Dong, E. Di Fabrizio, M. B. Yu, and G. Q. Lo, "Evolution of modes in a metal-coated nano-fiber," Opt. Express **19**(25), 25206–25221 (2011).
16. A. Mohammadi and M. Agio, "Light scattering under nanofocusing: toward coherent nanoscopies," Opt. Commun. **285**(16), 3383–3389 (2012).

#173351 - $15.00 USD Received 26 Jul 2012; revised 29 Oct 2012; accepted 5 Nov 2012; published 20 Dec 2012

17. A. A. Mikhailovsky, M. A. Petruska, M. I. Stockman, and V. I. Klimov, "Broad band near-field interference spectroscopy of metal nanoparticles using a femtosecond white-light continuum," Opt. Lett. **28**(18), 1686–1688 (2003).
18. X. W. Chen, V. Sandoghdar, and M. Agio, "Nanofocusing radially-polarized beams for high-throughput funneling of optical energy to the near field," Opt. Express **18**(10), 10878–10887 (2010).
19. F. De Angelis, R. P. Zaccaria, M. Francardi, C. Liberale, and E. Di Fabrizio, "Multi-scheme approach for efficient surface plasmon polariton generation in metallic conical tips on AFM-based cantilevers," Opt. Express **19**(22), 22268–22279 (2011).
20. F. De Angelis, F. Gentile, F. Mecarini, G. Das, M. Moretti, P. Candeloro, M. L. Coluccio, G. Cojoc, A. Accardo, C. Liberale, R. P. Zaccaria, G. Perozziello, L. Tirinato, A. Toma, G. Cuda, R. Cingolani, and E. Di Fabrizio, "Breaking the diffusion limit with super-hydrophobic delivery of molecules to plasmonic nanofocusing SERS structures," Nat. Photonics **5**(11), 682–687 (2011).
21. R. P. Zaccaria, F. De Angelis, A. Toma, L. Razzari, A. Alabastri, G. Das, C. Liberale, and E. Di Fabrizio, "Surface plasmon polariton compression through radially and linearly polarized source," Opt. Lett. **37**(4), 545–547 (2012).
22. M. I. Stockman, "Nanofocusing of optical energy in tapered plasmonic waveguides," Phys. Rev. Lett. **93**(13), 137404 (2004).
23. R. Proietti Zaccaria, A. Alabastri, F. De Angelis, G. Das, C. Liberale, A. Toma, A. Giugni, L. Razzari, M. Malerba, H. B. Sun, and E. Di Fabrizio, "Fully analytical description of adiabatic compression in dissipative polaritonic structures," Phys. Rev. B **86**(3), 035410 (2012).
24. K. C. Neuman and A. Nagy, "Single-molecule force spectroscopy: optical tweezers, magnetic tweezers and atomic force microscopy," Nat. Methods **5**(6), 491–505 (2008).
25. C. Liberale, P. Minzioni, F. Bragheri, F. De Angelis, E. Di Fabrizio, and I. Cristiani, "Miniaturized all-fibre probe for three-dimensional optical trapping and manipulation," Nat. Photonics **1**(12), 723–727 (2007).
26. F. De Angelis, C. Liberale, M. L. Coluccio, G. Cojoc, and E. Di Fabrizio, "Emerging fabrication techniques for 3D nano-structuring in plasmonics and single molecule studies," Nanoscale **3**(7), 2689–2696 (2011).
27. www.lumerical.com
28. www.cst.com
29. G. Baffou, R. Quidant, and F. J. García de Abajo, "Nanoscale control of optical heating in complex plasmonic systems," ACS Nano **4**(2), 709–716 (2010).
30. J. N. Israelachvili, *Intermolecular and surface forces* (Academic Press, 2010).
31. H. Hövel, S. Fritz, A. Hilger, U. Kreibig, and M. Vollmer, "Width of cluster plasmon resonances: bulk dielectric functions and chemical interface damping," Phys. Rev. B Condens. Matter **48**(24), 18178–18188 (1993).
32. S. J. Youn, T. H. Rho, B. I. Min, and K. S. Kim, "Extended Drude model analysis of noble metals," Phys. Status Solidi, B Basic Res. **244**(4), 1354–1362 (2007).

Nanostructuring techniques allow the fabrication of a large variety of materials with a fine control on their geometries and chemical composition, down to atomic scales. The ability of researchers to design complex nanostructures capable of providing the desired optical and electronic properties is still expected to increase. The characteristics required in a nanomaterial synthesis are the detailed control of the final product in term of size, shape, and chemical composition, and although many efforts are done, significant uncontrolled results are still not unusual. Under this point of view, the capability of determining the local optical properties of nanomaterials is essential for a number of practical applications but also for data interpretation, theoretical design and parameters optimization. One of the main hurdles is the lack of a tool capable of providing a deep characterization of the local optical response at the nanoscale. In fact, at the present the local or individual optical properties of nanostructured materials are poorly known or completely unknown. Therefore, it would be desirable to have the capability of their measurement.

Optical forces induced by surface plasmon polariton have been widely studied as a tool for trapping and manipulating nano-objects [1–6]. Here we propose a plasmonic based force spectroscopy capable to investigate the local optical parameters. The proposed tool is based on force measurements performed by combining Atomic Force Microscopy (AFM) and Plasmonics [7–17]. The working principle of the technique is sketched in Fig. 1(a). A silver nanocone is fabricated on an AFM cantilever, and when it is illuminated under the proper conditions [18–21] surface plasmon polaritons are launched from the base of the nanocone toward the tip, where the adiabatic compression of the electric field occurs [22,23]. Next, the strong electric field originating between the tip and substrate generates an attractive force whose intensity is calculated hereafter.

#173351 - $15.00 USD Received 26 Jul 2012; revised 29 Oct 2012; accepted 5 Nov 2012; published 20 Dec 2012

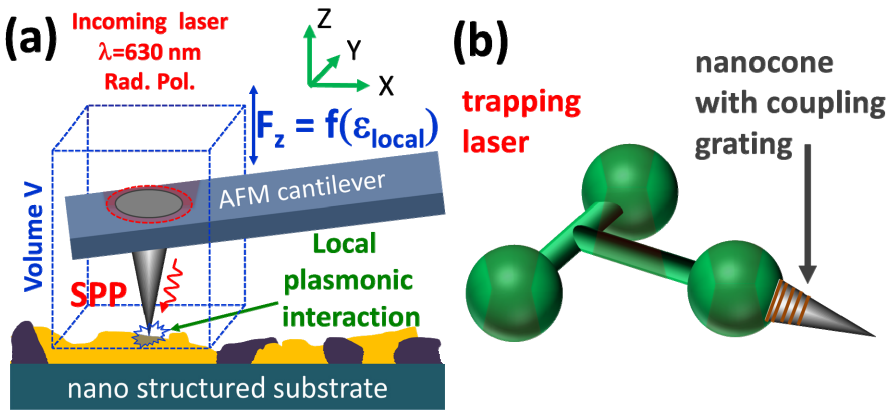

Fig. 1. Sketch of the device: plasmonic conical probe mounted an AFM cantilever (a), or integrated on modified beads for optical trapping (b).

Among several applications of AFM microscopy [24], atomic force spectroscopy is recently emerged as a powerful characterization technique for mechanical studies of many different micro and nano structured materials, including biological surface, tissues, or even single molecules (pulling force on protein, polymers, DNA). Under optimized conditions, force measurements in the piconewton range or below [14] are actually achievable, and this sensitivity limit is expected to lower in the next years. However, when optical tweezers are exploited [25], force measurements can be performed even in the femtonewton regime [24]. We already proposed [26] a nanostructured tripod that combines optical trapping with a plasmonic probe. The device is sketched in Fig. 1(b) and, among the different possible applications, it could be ideal for the implementation in liquid environment, especially when complex surfaces with 3D topographies have to be studied.

By employing Finite Difference Time Domain (FDTD) approach [27] we performed three-dimensional numerical calculations of the interaction forces existing between the plasmonic tip and different surfaces. These optical forces acting on the nanocone can be accurately calculated using the Maxwell Stress Tensor (MST) formalism [2,3]. We found that: i) these forces depend on the local optical response of the investigated materials with a resolution comparable to the radius of curvature of the tip or below; ii) the forces range is accessible to the current AFM and optical tweezers technology; iii) the force exhibits a clear dependence on both imaginary and real part of the materials permittivity. Therefore, these findings can be exploited to determine the local permittivity of a nanostructured material with a spatial resolution of few nanometers. We emphasize that to our knowledge, none of the techniques currently used to investigate the dielectric permittivity or refraction index, are able to determine the local response of a system at the nanoscale.

In order to obtain a realistic evaluation of the interaction forces, we considered a nanocone with a base of 300 nm, a height of 2 μm, and a tip with a curvature radius equal to 10 nm (smaller tips induce stronger forces but are very difficult to be fabricated and used). The cone is made of silver ($\varepsilon_{real} = -15.7$; $\varepsilon_{imag} = 1.06$, at $\lambda = 630$nm, Palik database) and it is illuminated with a radially polarized laser beam travelling parallel to the cone axis and impinging at the cone base. The beam spot size is around 600 nm, and it mimics an objective with numerical aperture equal to 0.6. Under this condition, an optical coupling between laser and nanocone of 7% in power is obtained, whereas for higher numerical aperture, optical coupling up 80% has been predicted [15]. Indeed, as we already reported, also a linear polarization with or without the help of a Photonic Crystal cavity, can be exploited to accumulate high electric field at the tip end (roughly 30% lower than that of radial polarization) while simplifying the experimental setup [7,8]. The mesh size in the critical region (the tip end and the substrate interface close to the tip) is set to 0.25 nm. With this

#173351 - $15.00 USD Received 26 Jul 2012; revised 29 Oct 2012; accepted 5 Nov 2012; published 20 Dec 2012

choice we can study tip of 10 nm radius of curvature and tip-substrate gap down to 1 nm having no significant grid problems.

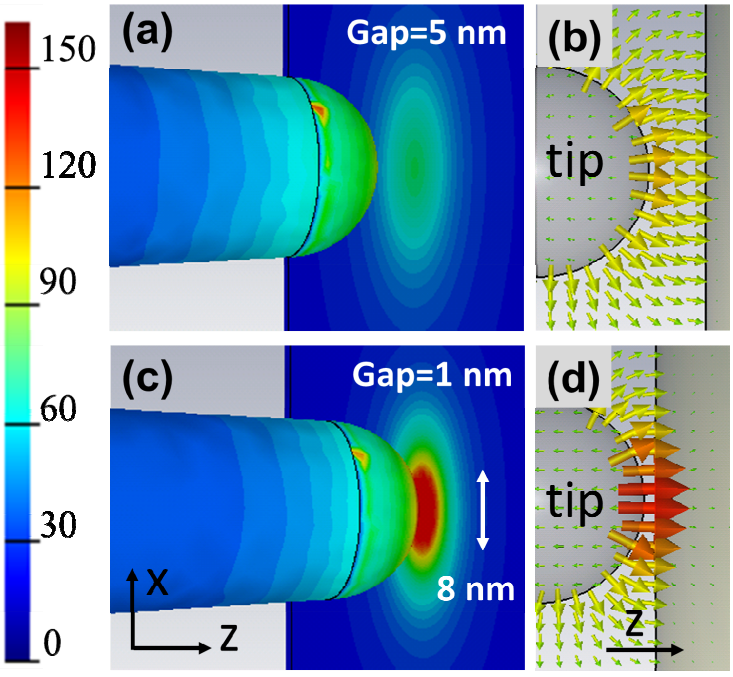

Fig. 2. (a,b) Plasmonic probe excited with a radial polarized laser approaching a dielectric surface (ε = 4), when the gap is 5 nm (a) and 1 nm (b). (c,d) Electric field vectors corresponding to (a) and (b) respectively. The electric field scale is with respect of source field amplitude.

The numerical calculations were also performed by employing different software package [28] obtaining comparable results (not reported for brevity). As introduced, we used the MST to calculate the optical forces acting on the nanocone:

$$F_\alpha = \oint_S \sum_\beta \frac{1}{2} \mathrm{Re}\left(T_{\alpha\beta}\hat{n}_\beta\right) dS \tag{1}$$

$$T_{\alpha\beta} = \varepsilon E_\alpha E_\beta^* + \mu H_\alpha H_\beta^* - \frac{1}{2}\delta_{\alpha\beta}\left(\varepsilon|E|^2 + \mu|H|^2\right) \tag{2}$$

where F_α is component α of the force, $T_{\alpha\beta}$ is the Maxwell Stress Tensor, $\hat{n}_\beta$ is component β of the outward unit vector normal to the surface S that surrounds the volume V (see Fig. 1), and $\delta_{\alpha\beta}$ is the Kronecker tensor. In absence of the substrate, (isolated nanocone plus cantilever in air) the simulation returns a total force directed parallel to the z axis: $Fz \approx$1-2 fN/μW (forces are normalized with respect to the incident laser power). The analysis shows that the force is mainly due to the z component of the electric field at the tip end, whereas the magnetic contribution is negligible.

The physical meaning of the MST relies on the difference between the incoming and outgoing linear momentum (the wave-vector k=2π/$\lambda_{plasmon}$), with respect to the volume V on which the force acts, i.e. $F \propto \left|\vec{k}^{out} - \vec{k}^{in}\right|$. When the tip approaches the sample surface, the plasmonic interaction between tip and substrate causes a rotation of $\vec{k}^{out}$ that is now mainly

#173351 - $15.00 USD Received 26 Jul 2012; revised 29 Oct 2012; accepted 5 Nov 2012; published 20 Dec 2012

directed toward the substrate, i.e. $\vec{k}_z^{\,out}$ increases at the expenses of $\vec{k}_{x,y}^{\,out}$ where $\vec{k}^{out} = \vec{k}_x^{\,out} + \vec{k}_y^{\,out} + \vec{k}_z^{\,out}$. Since the longitudinal force is given by $F_z \propto \left|\vec{k}_z^{\,out} - \vec{k}_z^{\,in}\right|$, this rotation of $\vec{k}^{out}$ (i.e. increases of $\vec{k}_z^{\,out}$) causes an increasing of the longitudinal component of the forces F_z. On the contrary, the force in the *xy* plane has a zero resultant by symmetry and it plays a minor role. In a similar picture, as shown in Fig. 2, the longitudinal component of the electric field E_z increases at expenses of the radial components E_x and E_y which, in turn, causes an increasing of the longitudinal component of force. This finding can be better understood by analyzing the MST structure: since the electric field at the tip apex is 2-3 orders of magnitude higher than in other nanocone regions, we can neglect the electric field components outside the tip end. Under this condition the Eq. (1) and Eq. (2) return the longitudinal force as:

$$F_z \cong \varepsilon_r \int_S \left(E_z^2 - E_x^2 - E_y^2\right) dS \equiv \varepsilon_r I_{MST} \tag{3}$$

Here *S* denotes the interface between the tip and the substrate, and ε_r is the permittivity of the medium surrounding the nanocone. Looking at the Eq. (3), it is clear that F_z increases with E_z at the expenses of $E_{x,y}$. In this calculations, the nanocone is surrounded by silicon nitride ($\varepsilon_r = 4$) at the base, and air ($\varepsilon_r = 1$) all around (including the tip apex).

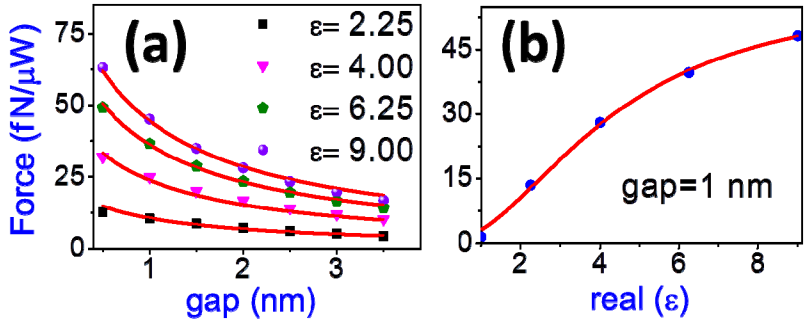

Fig. 3. (a) Force acting on the nanocone as function of the gap-substrate distance for substrates with different dielectric constants. (b) Force acting on the nanocone as function of the dielectric constant of the substrate (gap 1nm). Forces values are normalized with respect of incident laser power. For fitting functions details see text.

In Fig. 3(a) is reported the force acting on the nanocone when the cantilever approaches a dielectric substrate (forces are attractive; tip radius 10 nm, laser power 1μW, λ = 630 nm, $\varepsilon_{dielectric} = 2.25 \div 9$). The graph shows a hyperbolic behavior with respect to tip-substrate gap distance, which is very similar to the dipolar-like interaction between a metallic nanoparticle and a flat substrate. We fitted the data with the function:

$$F(z,\varepsilon) = A\frac{1}{z+z_0}\frac{\varepsilon^2}{K+\varepsilon^2} \tag{4}$$

founding a good agreement between data and model (A = 102 fN, z_0 = 0.8 nm, K = 18.4, z = gap). In Fig. 3(b), we reported the force acting on the nanocone when a dielectric substrate of increasing permittivity is placed at fixed distance from the tip (1nm). For low values ($\varepsilon < 4 \div 5$) the calculated forces (blue dots in Fig. 3(b)) exhibit a linear trend whereas for higher values they exhibit a plateau. The data are fitted with the same function of Eq. (4), where z = 1nm, i.e. $56.7\frac{\varepsilon^2}{18.4+\varepsilon^2}$ (fitting curve is plotted in red).

#173351 - $15.00 USD Received 26 Jul 2012; revised 29 Oct 2012; accepted 5 Nov 2012; published 20 Dec 2012

To further investigate the capabilities of this approach, we considered the interaction between the plasmonic tips and noble metals. In Fig. 4 is reported the optical force calculated for a silver nanocone interacting with a noble metal substrate. Figure 4(a): the force with respect to the real part of the permittivity while the imaginary part is kept constant (ε_{imag} = 1.36); Fig. 4(b): the force as a function of the imaginary part of the permittivity while the real part is kept constant (ε_{real} = −16). In both cases the optical force exhibits an exponential behavior spanning from few tenths up to hundreds of fN per μW of incident laser beam power.

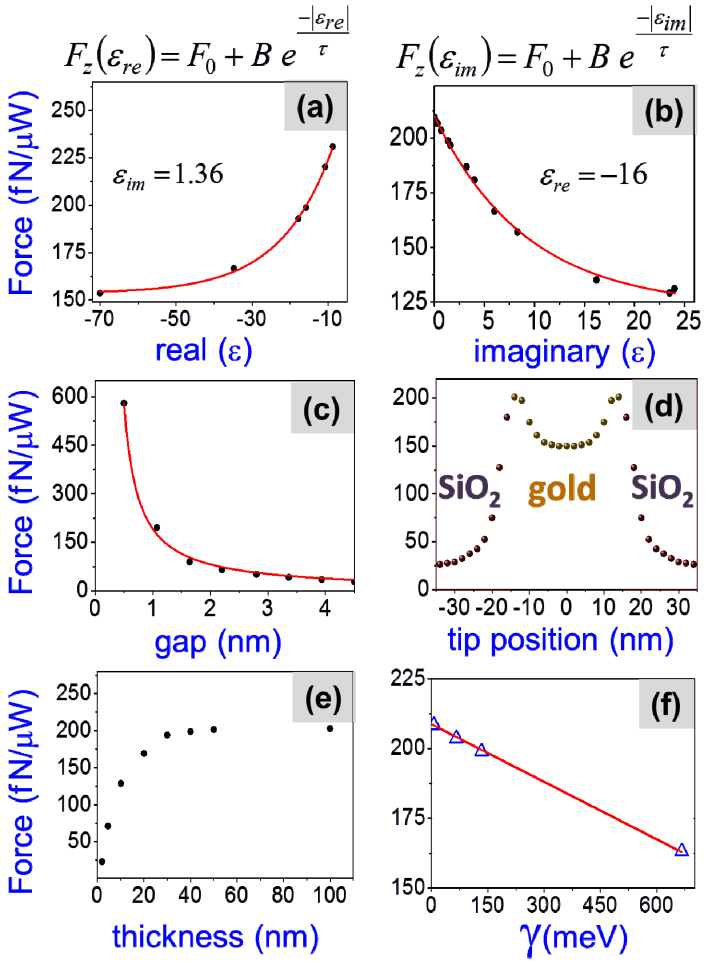

Fig. 4. (a,b,c,) Force acting on the nanocone with respect to the real part of ε (a), imaginary part of ε (b), tip-substrate gap (c). (d) Force obtained when the tip scans a gold stripe (WxHxL = 30x30x500 nm) on silicon oxide substrate. (e) Force with respect of substrate thickness, when substrate is gold with a dielectric supporting layer. (f) Force with respect of damping constant γ (substrate is noble metal with ε_{ion} = 3.8, and ω_{plasma} = 8eV).

In currently available AFM system, the minimum force sensitivity is limited by the thermal fluctuations [14], which be calculated from $F_{min} = [(4k_BT\ k\ W)/\omega_0 Q]^{1/2}$ where k_B is the Boltzmann constant, T is the room temperature, k is the spring constant of the cantilever (≈few N/m), W is the bandwidth of measurement (set by lock-in amplifier) used in the force measurement (≈10 Hz), ω_0 is the resonant frequency of the AFM tip (:100 kHz), and Q is the quality factor of the cantilever (:160). This leads to a force sensitivity on the order of:50 fN. Thus, measuring optical forces on the order of a fraction of piconewton is actually possible

#173351 - $15.00 USD Received 26 Jul 2012; revised 29 Oct 2012; accepted 5 Nov 2012; published 20 Dec 2012

and not limited by the thermal sensitivity. In our case, an incident laser power of few μW is sufficient to induce plasmonic forces greater than 1pN that is far above the current limitations. Furthermore, higher plasmonic forces can be obtained for the same laser power by improving the coupling efficiency, which we remind to be only 7% in the present optical setup, namely much lower than the theoretical limit of 80% [15].

Concerning the device heating, in view of the data already available in literature [29], for low laser power (up to few tenths of μW) the nanocone temperature should increase of no more than few degrees which should not affect the device functioning.

Finally, we fitted the data in Fig. 4 with the exponential function:

$$F = F_0 + B\exp\left(\frac{-|\varepsilon|}{\tau}\right) \tag{5}$$

For graph 4(a): $F_0 = 122$, $B = 87$, $\tau = 9.2$; for graph 4(b): $F_0 = 153$, $B = 146$, $\tau = 13$. In Fig. 4(c) is reported the force acting on the nanocone as a function of tip-substrate gap for a gold substrate ($\varepsilon_{real} = -9.1$; $\varepsilon_{imag} = 1.28$). As it can be seen, forces values well above the current sensitivity range (50 fN for AFM setup, and less for OT) can be obtained with a laser power of few μW and gaps of few nm. We notice that Van der Waals forces, or other kinds of interactions, could be comparable with the plasmonic forces for the cases we considered [30]. However, these contributions can be estimated by means of a static force measurement, and then subtracted.

To evaluate the spatial resolution of the proposed plasmonic force microscope, we simulated the force acting on the nanocone when it scans a gold nanostripe (W × H × L = 30x30x500 nm) on a SiO_2 substrate. The resulting forces are reported in Fig. 4(d). As it can be seen, the spatial resolution is in the order of 5 nm that is far below the tip size (20 nm). This is due to the fact that the plasmonic field responsible for the optical force is enhanced only at the tip apex, where it faces the substrate (see also Fig. 2(d)). This graph shows how the proposed Plasmonic Force Microscopy can be used for providing additional information regarding the nature of surface under investigation in addition to topographical information provided by conventional scanning probe microscopy. For instance, one could use this tool to discriminate a metallic features from dielectric ones during AFM topographies. We notice that for adiabatic plasmonic probes with smaller tip size, the plasmonic field experiments an additional accumulation with respect to standard TERS, that causes a further increasing of both optical forces and spatial resolution.

Finally, we found that the interaction between the tip and the substrates happens in a length scale dictated by the skin depth. In Fig. 4(e), we reported the force as a function of the Gold layer thickness. For metal layers thicker than 30 nm (comparable to the skin depth of noble metal in the visible range), the force measurement is no longer sensible to a further increase of the metal thickness.

The data reported in Figs. 2-4 confirm the three main statements on which the proposed plasmonic force microscope relies: i) local sensing; ii) range of magnitude accessible to current force measurements techniques; iii) clear dependence of the forces on the substrate optical permittivity. From the fit, it will be possible to calculate the local dielectric response by measuring the optical force on a well-known isotropic substrate (such as silicon nitride, silicon oxide, or crystalline gold). Once the fitting parameters (A, z_0, and K for dielectric model) have been estimated, plasmonic force measurements can be carried out on the desired substrate to evaluate its local dielectric function. This approach is valid for the evaluation of the real part of dielectric substrate, when imaginary part can be neglected (the majority of common dielectric materials). However, the situation can be extended to metals where the force is affected from both real and imaginary part.

To obtain both the real and the imaginary part of the permittivity, some hypothesis have to be done either on the former or the latter. For instance, let us consider the Drude-Lorentz model:

#173351 - $15.00 USD Received 26 Jul 2012; revised 29 Oct 2012; accepted 5 Nov 2012; published 20 Dec 2012

$$\varepsilon(\omega) = \varepsilon_{ionic} + \left(\frac{i\omega_{plasma}^2}{\omega(\gamma - i\omega)} \right) \quad (6)$$

where ε_{ionic} is the ionic contribution, γ is the damping constantr, and ω_{plasma} is the plasma frequency ($\omega_{plasma}^2 = \frac{ne^2}{m}$ where *n, e*, and *m*, are the electron density, charge and electron mass, respectively).

Deviations from the Drude-Lorentz model can be taken into account by including into the damping constant γ the contributions coming from electron scattering events following the rule $\gamma_{total}^{-1} = \sum_i \gamma_i^{-1}$ (scattering with electrons, phonons, surface, defects, etc.). However, other models can also be considered depending on the case [31]. As example of how the local dielectric response can be determined in metal nanostructures, we assume that for nanostructured materials both the plasma frequency and the ionic contribution are the same as in bulk materials, and the variation of the dielectric permittivity $\varepsilon(\omega)$ is determined only by one parameter, i.e. the damping constant γ, that is supposed to include the deviations from the ideal Drude-Lorentz case.

We calculated the dependence of the plasmonic force on the damping constant of the metallic substrate. For the ionic contribution and the plasma frequency we chosen the values equal to 3.8 and 8 eV, respectively (these values are in the range of noble metals [32]). In Fig. 4(f) is reported the optical force with respect to γ: it exhibits a very good linear trend over a wide range of γ values (from 6.5 to 650 meV). Now the force depends only on one single parameter (damping constant γ) and then it can be used to estimate ε. We point out that for each plotted point of Fig. 4(f), both ε_{real} and ε_{imag} change from point to point. This characteristic does not affect the linear trend and, to our knowledge, it represents an additional interesting finding that deserves to be further investigated.

More in general, further theoretical investigations are necessary to understand this behavior and in particular, analytical solutions of the interaction between the plasmonic probes and substrates are desirable to fully exploit this approach. Moreover, such a theoretical model should take in account quantum effects which are expected to appear for very low tip-substrate gap (below 1nm).

In conclusion, we presented three dimensional numerical calculations concerning the optical force acting on a plasmonic tip when it interacts with dielectric or metallic substrate. The plasmonic probe can be mounted on an AFM cantilever or on 3D structured beads (tripod), to be combined with scanning probe technology or optical tweezers, respectively. We showed that the optical forces caused by the plasmonic field depend on the local response of the substrates. In principle this plasmonic force microscopy is able to probe both the real and the imaginary part of the local dielectric function ε with a spatial resolution of few nanometers. We found that, under experimental realistic conditions, the optical forces are in a range of sensitivity accessible to the current *state of the art* force measurements. This approach promises to open the route to the characterization of dielectric response of nanostructured materials at the nanoscale.

#173351 - $15.00 USD Received 26 Jul 2012; revised 29 Oct 2012; accepted 5 Nov 2012; published 20 Dec 2012